Available online at www.sciencedirect.com
ScienceDirect
Journal of Power Sources 179 (2008) 541–546
JOURNAL OF POWER SOURCES
www.elsevier.com/locate/jpowsour

Short communication

Catalytic modification of Ni–Sm-doped ceria anodes with copper for direct utilization of dry methane in low-temperature solid oxide fuel cells

Zhicheng Wang, Wenjian Weng *, Kui Cheng, Piyi Du, Ge Shen, Gaorong Han

Department of Materials Science and Engineering, Zhejiang University, Hangzhou 310027, PR China

Received 7 January 2008; accepted 10 January 2008
Available online 1 February 2008

Abstract

A Cu/Ni/Sm-doped ceria (SDC) anode has been designed for direct utilization of dry methane in low-temperature anode-supported solid oxide fuel cells. The anode is prepared by the impregnation method, whereby a small amount of Cu is incorporated into the previously prepared Ni/SDC porous matrix. After reduction, Cu nanoparticles adhere to and are uniformly distributed on the surface of the Ni/SDC matrix. For the resulting Cu/Ni/SDC anode-supported cell, maximum power density of 317 mW cm^{-2} is achieved at 600 °C. The power density shows only ~2% loss after 12-h operation. The results demonstrate that the Cu/Ni/SDC anode effectively suppresses carbon deposition by decreasing the Ni surface area available and the level of carbon monoxide disproportionation. This combination of effects results in very low-power density loss over the operating time.

Keywords: Solid oxide fuel cells; Cu/Ni/SDC anode; Impregnation method; Dry methane; Operational stability; Carbon deposition

1. Introduction

In comparison with conventional solid oxide fuel cells (SOFCs) that use H_2, low-temperature SOFCs that involve direct hydrocarbon oxidation have several advantages, including higher fuel efficiency, lower cost and no reforming process [1–4]. However, carbon deposition on Ni-based anodes due to Ni-catalyzed hydrocarbon decomposition [5] may rapidly degrade the SOFC performance. Hence, an anode with strong ability to suppress carbon deposition is critical in the design of SOFCs operated with hydrocarbon [6,7].

One approach for inhibiting carbon deposition is to replace Ni in the anode by other metals on condition that the electrochemical catalytic activity and electronic conductivity are maintained. However, the choices are limited. Some metals, such as Co and Fe, show good electrochemical catalytic activity, but suffer from similar carbon decomposition problems [8,9]. Noble metals are expensive for anode use in large amounts. Some conducting oxides, such as $La_{0.8}Ca_{0.2}CrO_3$ and $Ce_{0.9}Gd_{0.1}O_{1.95}$ [10], have electronic conductivity values that are too low to meet SOFC requirements, even though their electrochemical reactivity and carbon deposition inhibition are excellent.

Cu is relatively inert for carbon formation during electrochemical oxidation of hydrocarbons. However, the electrochemical catalytic activity of Cu is inferior to that of Ni [11] and the low-melting temperature of CuO_x means that Cu-based anodes are not very feasible. A practical approach to combining good electrochemical catalytic activity and effective inhibition of carbon deposition is to incorporate a small amount of Cu into a Ni-based anode. Xie et al. [6] prepared a $Ni_{0.95}Cu_{0.05}/Ce_{0.8}Sm_{0.2}O_{1.9}$ (SDC) anode-supported cell operated with hydrocarbon at low temperature. Fairly good performance was achieved and the carbon deposition rate was relatively low, but carbon was still formed on the anode. Further improvement of Cu–Ni bimetal anodes in terms of their capability to suppress carbon deposition is still necessary.

In the present study, a novel anode was designed for direct operation with hydrocarbons. This anode is based on a porous Ni/SDC cermet modified with a small amount of Cu nanoparticles. The Cu nanoparticles were uniformly distributed on the

* Corresponding author. Tel.: +86 571 87953787; fax: +86 571 87953787.
E-mail addresses: wzc877@zju.edu.cn (Z. Wang), wengwj@zju.edu.cn (W. Weng), chengkui@zju.edu.cn (K. Cheng), dupy@zju.edu.cn (P. Du), sg@zju.edu.cn (G. Shen), hgr@zju.edu.cn (G. Han).

0378-7753/$ – see front matter © 2008 Elsevier B.V. All rights reserved.
doi:10.1016/j.jpowsour.2008.01.040

pore walls of the cermet to form a Cu/Ni/SDC anode. For this proposed anode, it is expected that carbon deposition will be effectively suppressed because the role of Cu is maximized and SDC itself can inhibit carbon formation. Furthermore, Ni–Cu [11,12] and SDC–Cu [7] interactions in the anode can promote catalysis of carbon monoxide oxidation, which has also a positive effect on suppressing carbon formation [3]. Here, we report on such a Cu/Ni/SDC anode that was prepared by an impregnation method. The resulting Cu/Ni/SDC-supported cell was tested at 600 °C with dry CH_4 as fuel. For comparison, Ni/SDC and $Ni_{0.95}Cu_{0.05}$/SDC anodes were also prepared and tested in cells under the same conditions. The possible mechanism for Cu/Ni/SDC suppression of carbon deposition is discussed.

2. Experimental

2.1. Powder preparation

Nanosized SDC, NiO/SDC, $Ni_{0.95}Cu_{0.05}O$ and $Sm_{0.5}Sr_{0.5}CoO_3$ (SSC) powders were synthesized by the glycine–nitrate process [13,14]. Stoichiometric amounts of the precursors $Ce(NO_3)_4{\cdot}6H_2O$ (99.9%) and $Sm(NO_3)_3{\cdot}6H_2O$ (99.9%) were dissolved in deionized water. Then glycine was added with stirring. The molar ratio of NO^{3-} to glycine was 2. The resulting solution was heated to evaporate excess free water, and the residual viscous resin transformed to a dark-brownish foam on heating. When heated further, spontaneous ignition occurred, and a voluminous, pale-yellow, sponge-like SDC ash was obtained. The SDC ash was subsequently fired at 700 °C for 2 h to yield SDC powder. The other powders were prepared using a similar procedure. SSC powder was mixed with 30 wt.% SDC powder by wet ball-milling for 72 h as the cathode material. $Ni_{0.95}Cu_{0.05}O$ powder was mixed with 35 wt.% SDC powder by wet ball-milling for 72 h as the anode material. Ethanol was used as the liquid medium for ball-milling.

2.2. Single cell fabrication

To prepare Cu/Ni/SDC anode-supported cells, NiO/SDC powder was mixed with polystyrene (10 wt.%) foaming agent [15] and first pressed at 100 MPa into a disc (~15 mm in diameter and 1 mm in thickness). Then SDC powder was placed on top and pressed at 200 MPa to yield a bilayer disc [16]. The bilayer was subsequently fired at 1350 °C for 4 h and reduced in flowing H_2 at 600 °C for 4 h. Cu was added to the porous Ni/SDC cermet by impregnation in an aqueous solution containing copper nitrate and urea at a 1:1.5 molar ratio [17]. The deposited copper salts were reduced to Cu metal in flowing H_2 at 500 °C. The Cu/Ni molar ratio was 1:19 and Cu loading was controlled by the number of times impregnation was carried out. In the present study, the molar ratio of different metal elements in the Cu/Ni/SDC anode was the same as that in the $Ni_{0.95}Cu_{0.05}$/SDC anode. A slurry consisting of SSC/SDC (30 wt.% SDC) and ethylcellulose was then spin-coated onto the electrolyte surface and subsequently fired at 950 °C in air for 2 h to form a porous cathode.

Ni/SDC (35 wt.% SDC) and $Ni_{0.95}Cu_{0.05}$/SDC (35 wt.% SDC) supported cells with thin SDC electrolytes were prepared using a similar procedure, but without impregnation. To avoid variations in resistance due to cathodic polarization, all the cathodes were fabricated using the same processes. All the single cells consisted of a ~20-μm SSC–SDC cathode, a ~20-μm SDC electrolyte and a ~550-μm anode.

2.3. Cell testing

The single cells were mounted onto a quartz tube. Silver paste was used to seal the anode compartment. A silver current collector was fabricated on the cathode surface by painting a circular pattern in the center of the cathode using silver paste [18]. Two silver wires were attached to the anode and the cathode with silver paste. The single cells were tested at 600 °C and the anode and cathode were fed with dry CH_4/air as fuel/oxidant. Current density–voltage (*I–V*) relationships were determined for the cells using a potentiostat (CHI600C, CH Instruments) with a constant fuel flow rate of 60 cm^3 min^{-1} at room temperature. The impedance of the cell under open-circuit conditions was measured in the frequency range from 0.01 Hz to 100 kHz with 5 mV as the excitation ac amplitude using an ac impedance spectroscope interfaced to a computer. The microstructure of the prepared electrodes was observed using a field emission scanning electron microscope (FESEM, model SIRION-100, FEI). The conductivity of the different anodes was measured using the four-probe method [19]. Carbon deposition after testing was analyzed using an energy-dispersive spectroscopy (EDS) attachment.

3. Results and discussion

3.1. Anode characterization

The XRD pattern of the Ni/SDC anode (Fig. 1a) only shows diffraction peaks for Ni and SDC phases. After Cu incorporation

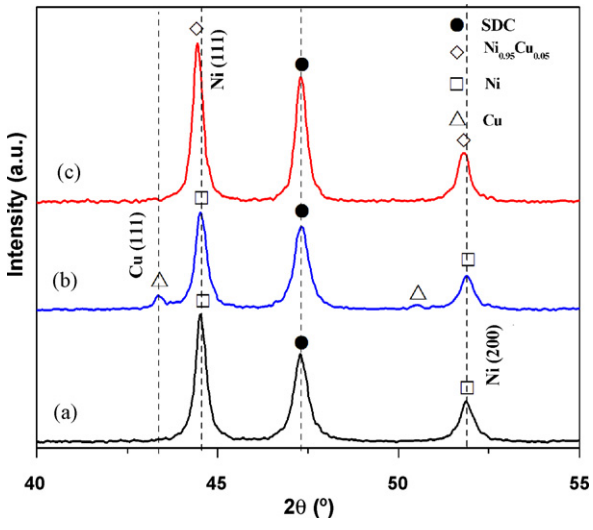

Fig. 1. XRD patterns of the (a) Ni/SDC, (b) Cu/Ni/SDC and (c) $Ni_{0.95}Cu_{0.05}$/SDC anodes.

into the anode by impregnation and reduction, an additional Cu phase appeared (Fig. 1b), confirming that a Cu/Ni/SDC anode was obtained. The XRD pattern of the $Ni_{0.95}Cu_{0.05}$/SDC anode (Fig. 1c) shows diffraction peaks attributed to the (1 1 1) and (2 0 0) planes of the fcc structure of Ni, with no Cu phase. Furthermore, the fcc peaks are at lower angles compared to those for the Ni-based anode (Fig. 1a), indicating that $Ni_{0.95}Cu_{0.05}$ alloy was formed.

The SEM micrograph (Fig. 2a) and the corresponding copper map (Fig. 2b) for the Cu/Ni/SDC anode confirm that Cu particles were distributed uniformly on the porous Ni/SDC matrix.

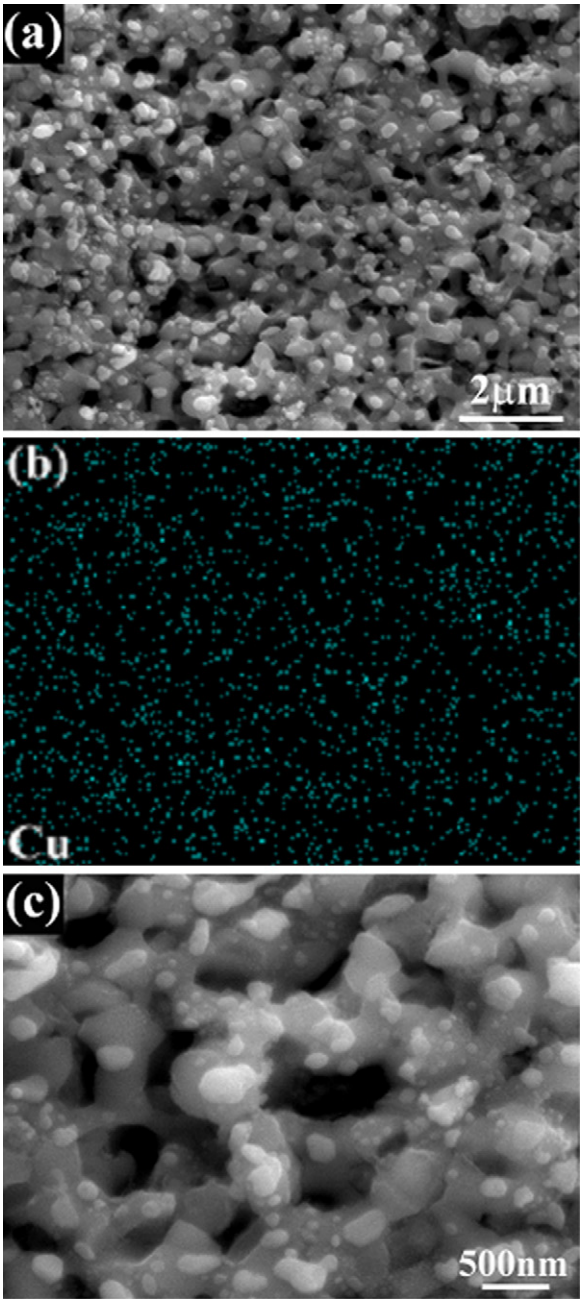

Fig. 2. (a) SEM image of the porous Ni/SDC matrix after impregnation with Cu, (b) EDS mapping of the Cu distribution in (a) and (c) higher resolution of the SEM image in (a).

Table 1
Conductivity of the different anodes at 600 °C

Anode	Conductivity (S cm^{-1})
Ni/SDC	405
$Ni_{0.95}Cu_{0.05}$/SDC	417
Cu/Ni/SDC	633

The higher-magnification micrograph (Fig. 2c) shows that the impregnated Cu particles adhered well to the surface of the Ni/SDC matrix and that the particle size of Cu ranged from 50 to 250 nm.

The electronic conductivity at 600 °C (Table 1) is almost the same for the Ni/SDC and $Ni_{0.95}Cu_{0.05}$/SDC anodes, whereas the conductivity of the Cu/Ni/SDC anode is approximately 50% higher. The higher conductivity of the Cu/Ni/SDC anode further indicates that the Cu nanoparticles adhered well to the porous Ni/SDC matrix, providing an effective passage for transport of more electrons from the electrochemical reaction sites and thus enhancing the power output of the cell.

3.2. Cell performance for direct oxidation of dry CH_4

Fig. 3 shows the voltage and power density as a function of current density for different anode-supported cells operated at 600 °C with dry CH_4 as fuel. The maximum power density for Ni/SDC-, $Ni_{0.95}Cu_{0.05}$/SDC- and Cu/Ni/SDC-supported cells was 240, 338 and 317 mW cm^{-2}, respectively. The power output of the Ni/SDC-supported cell is obviously lower than that of the Cu-containing anode-supported cells. This result agrees with that reported by Ringuedé et al. [20]. The open circuit voltage (OCV) for Ni/SDC-, $Ni_{0.95}Cu_{0.05}$/SDC- and Cu/Ni/SDC-supported cells was 0.852, 0.902 and 0.884 V, respectively, all of which are lower than the theoretical value of 0.943 V based on complete oxidation of methane [7]:

$$CH_4 + 4O^{2-} \rightarrow CO_2 + 2H_2O + 8e^- \quad (1)$$

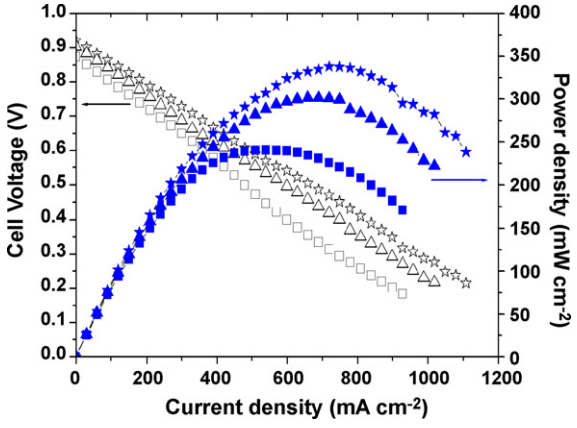

Fig. 3. Cell voltage (open symbols) and power density (solid symbols) as a function of current density at 600 °C for a Ni/SDC supported cell (square), a $Ni_{0.95}Cu_{0.05}$/SDC supported cell (star) and a Cu/Ni/SDC supported cell (triangle) with dry CH_4 as fuel.

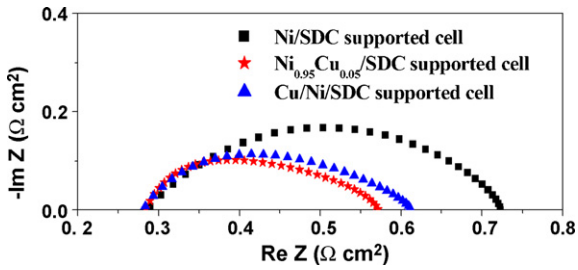

Fig. 4. Impedance spectra measured at 600 °C under open circuit conditions for a Ni/SDC supported cell (square), a $Ni_{0.95}Cu_{0.05}$/SDC supported cell (star) and a Cu/Ni/SDC supported cell (triangle) with dry CH_4 as fuel.

Such a result implies that incomplete oxidation [reaction (2)], and/or direct carbonization [reaction (3)] could occur:

$$CH_4 + O^{2-} \rightarrow CO + 2H_2 + 2e^- \quad (2)$$

$$CH_4 \rightarrow C + 2H_2 \quad (3)$$

The higher OCV for the Cu-containing anodes suggests that the presence of Cu in the anode can promote full electrochemical oxidation of CH_4 according to reaction (1).

The area-specific resistance (ASR), defined as the difference between the intercepts on the real axis at high and low frequency, is a combination of the anodic and cathodic interfacial polarization resistance [7]. According to the impedance spectra in Fig. 4, the ASR of Ni/SDC-, $Ni_{0.95}Cu_{0.05}$/SDC- and Cu/Ni/SDC-supported cells was 0.44, 0.29 and 0.33 $\Omega\,cm^2$, respectively. Since the cathodes and electrolytes in the three cells are identical, the differences in ASR mainly originate from the anodic interfacial polarization resistance. It can be concluded that the interfacial polarization resistance is very similar for the $Ni_{0.95}Cu_{0.05}$/SDC and Cu/Ni/SDC anodes, but lower than that of the Ni/SDC anode. This implies that small amounts of added Cu can decrease the anodic interfacial polarization resistance, which enhances the cell performance.

Both the *I–V* curves (Fig. 3) and impedance measurements (Fig. 4) demonstrate that a small amount of added Cu enhances the performance of Ni-based anodes. However, the performance of the Cu/Ni/SDC-supported cell is inferior to that of the $Ni_{0.95}Cu_{0.05}$/SDC cell. This could be because Cu particles on the surface of the Ni/SDC matrix decrease the Ni surface area available, as well as the triple-phase gas/Ni/SDC boundary length in the Cu/Ni/SDC anode, thus yielding lower cell performance. However, this is only the case during the initial stage of cell operation.

3.3. Cell stability during direct oxidation of dry CH_4

The time dependence of the maximum power density of the cells is shown in Fig. 5. As expected, the maximum power density of the Ni/SDC-supported cell decayed rapidly, with approximately 60% loss of the initial power density after 7 h of operation. The power output of $Ni_{0.95}Cu_{0.05}$/SDC-supported cell decreased more rapidly than that of the Cu/Ni/SDC-supported cell, although its initial maximum power density was higher. After 12 h, 7% of the initial power density was lost for the

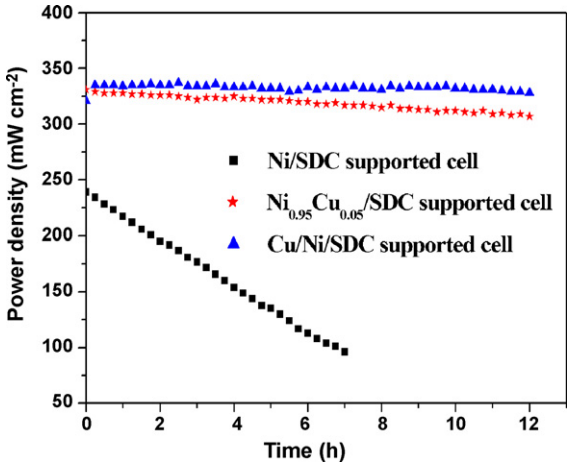

Fig. 5. Maximum power density of supported cells with different anodes operated at 600 °C with dry CH_4 as fuel.

$Ni_{0.95}Cu_{0.05}$/SDC-supported cell, whereas only 2% was lost for the Cu/Ni/SDC-supported cell. The results indicate that small amounts of added Cu efficiently increase the cell stability, and the presence of a single copper phase in the anode is even more favorable for improving the SOFC stability.

After testing, carbon formation on the anode surface was analyzed by EDS element mapping, as shown in Fig. 6. The relative carbon deposition area on the surface of the different anodes is summarized in Table 2 (DT-2000 image analysis system). The relative area on the anode reached approximately 49% for 7 h of operation of the Ni/SDC-supported cell using CH_4. The carbon covered almost all of the Ni surface, leading to a decrease in the triple-phase boundary length. Besides, the deposited carbon blocked the anode pores and obstructed gas transportation, resulting in an increase in the diffusion overpotential of the anode. All these directly lead to a progressive decrease in performance of the Ni/SDC-supported cell (Fig. 5). The Cu-containing anodes had significantly lower relative areas compared to the Ni/SDC anode, although carbon was still deposited on the anode matrix. Moreover, the Cu/Ni/SDC anode had the lowest amount of carbon deposition, which may result in more sustained power output from the cell than for the $Ni_{0.95}Cu_{0.05}$/SDC-supported cell. Obviously, the Cu nanoparticles in the Cu/Ni/SDC anode have a beneficial effect in suppressing carbon deposition and maintaining the stability of the cell.

According to other studies of CH_4-fuelled SOFCs, carbon deposition mainly occurs via two reactions, a pyrolysis reaction [reaction (3)] and carbon monoxide disproportionation via the so-called Boudouard reaction [3,21]:

$$2CO \rightarrow C + CO_2 \quad (4)$$

Table 2
Relative carbon deposition area on the surface of the different anodes

Anode	Operation time (h)	Relative carbon deposition area (%)
Ni/SDC	7	49
$Ni_{0.95}Cu_{0.05}$/SDC	12	13
Cu/Ni/SDC	12	5

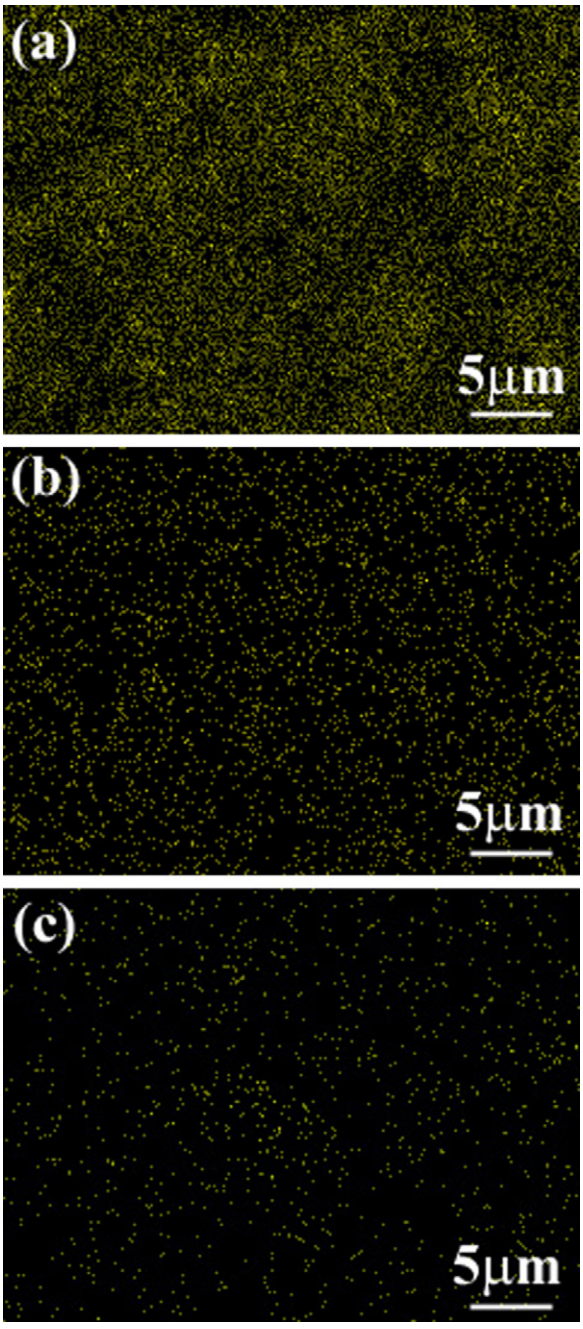

Fig. 6. EDS mapping of the carbon distribution on the anode surface: (a) Ni/SDC, (b) $Ni_{0.95}Cu_{0.05}$/SDC and (c) Cu/Ni/SDC.

Reaction (3) generally occurs at >700 °C [3]. Reaction (4) is exothermic, and its thermodynamic equilibrium is shifted to the right at lower temperature. Hence, it is considered that carbon formation according to the Boudouard reaction predominates with decreasing SOFC operating temperature [5].

As discussed above, the presence of Cu in the anode plays a very important role in suppressing carbon deposition. However, catalysis by $Ni_{0.95}Cu_{0.05}$ is similar to that by elementary Ni; methane decomposition [reaction (3)] is still catalyzed by the alloy to a certain extent. For the Cu/Ni/SDC anode, Cu particles are situated on the surface of the Ni/SDC matrix, which leads to more direct exposure of Cu to the fuel than on the $Ni_{0.95}Cu_{0.05}$/SDC anode. Hence, the Ni surface area available is decreased and less carbon deposition occurs on the Cu/Ni/SDC anode.

Furthermore, good interconnections among the three phases in the Cu/Ni/SDC anode allow Cu–Ni and Cu–SDC interactions. The former interaction can promote the water–gas shift reaction when H_2O is created during cell operation via reaction (1) [11]:

$$CO + H_2O \rightarrow CO_2 + H_2 \quad (5)$$

CO_2 generation decreases the CO/CO_2 ratio in the gas and additional hydrogen generation can increase the power output of the cell. Besides, Cu–SDC interaction exhibits higher activity for CO oxidation [22], which further decreases the CO/CO_2 ratio. Hence, suppression of carbon deposition according to reaction (4) in the Cu/Ni/SDC anode can be enhanced by these lower CO/CO_2 ratios.

4. Conclusions

A Cu/Ni/SDC anode was prepared by the impregnation method and reduction treatment. Impregnated Cu nanoparticles were connected to the surface of the porous Ni/SDC matrix. Such an anode shows better operational stability and catalytic activity when dry CH_4 is used as fuel. The corresponding cell shows excellent performance and better long-term stability of power density output than a cell with a $Ni_{0.95}Cu_{0.05}$ alloy anode. The better performance of the cell with the Cu/Ni/SDC anode is attributed to the presence of Cu nanoparticles in the anode, which greatly suppress carbon deposition during cell operation. First, the presence of Cu nanoparticles in the anode strengthens the role of Cu in suppressing carbon deposition. Second, good interconnections between the Cu nanoparticles and Ni and SDC enhance Cu–Ni and Cu–SDC interactions, which decreases carbon monoxide disproportionation.

References

[1] H. Tu, U. Stimming, J. Power Sources 127 (2004) 284–293.
[2] S. Park, J.M. Vohs, R.J. Gorte, Nature 404 (2000) 265–267.
[3] E. Perry Murray, T. Tsai, S.A. Barnett, Nature 400 (1999) 649–651.
[4] B. Zhu, J. Power Sources 93 (2001) 82–86.
[5] J.B. Wang, J.-C. Jang, T.-J. Huang, J. Power Sources 122 (2003) 122–131.
[6] Z. Xie, C. Xia, M. Zhang, W. Zhu, H. Wang, J. Power Sources 161 (2006) 1056–1061.
[7] W. Zhu, C. Xia, J. Fan, R. Peng, G. Meng, J. Power Sources 160 (2006) 897–902.
[8] R.J. Gorte, S. Park, J.M. Vohs, C. Wang, Adv. Mater. 12 (2000) 1465–1469.
[9] R.J. Gorte, J.M. Vohs, J. Catal. 216 (2003) 477–486.
[10] B.C.H. Steele, Nature 400 (1999) 619–620.
[11] T.-J. Huang, S.-Y. Jhao, Appl. Catal. A: Gen. 302 (2006) 325–332.
[12] T.-J. Huang, T.-C. Yu, S.-Y. Jhao, Ind. Eng. Chem. Res. 45 (2006) 150–156.
[13] S. Zha, W. Rauch, M. Liu, Solid State Ionics 166 (2004) 241–255.
[14] Y. Zhang, S. Zha, M. Liu, Adv. Mater. 17 (2005) 487–491.
[15] D. Zou, V. Derlich, K. Gandhi, M. Park, L. Sun, D. Kriz, Y.D. Lee, G. Kim, J.J. Aklonis, R. Salovey, J. Polym. Sci. A: Polym. Chem. 28 (1990) 1909–1921.
[16] C. Xia, M. Liu, Solid State Ionics 144 (2001) 249–255.
[17] S. Jung, C. Lu, H. He, K. Ahn, R.J. Gorte, J.M. Vohs, J. Power Sources 154 (2006) 42–50.
[18] M. Boder, R. Dittmeyer, J. Power Sources 155 (2006) 13–22.

[19] X. Fang, G. Zhu, C. Xia, X. Liu, G. Meng, Solid State Ionics 168 (2004) 31–36.
[20] A. Ringuedé, D.P. Fagg, J.R. Frade, J. Eur. Ceram. Soc. 24 (2004) 1355–1358.
[21] S.P. Yoon, J. Han, S.W. Nam, T.-H. Lim, J. Power Sources 136 (2004) 30–36.
[22] J.B. Wang, W.-H. Shih, T.-J. Huang, Appl. Catal. A: Gen. 203 (2000) 191–199.